Journal of Environmental Health Science and Engineering (2023) 21:403–416
https://doi.org/10.1007/s40201-023-00867-w

RESEARCH ARTICLE

Synthesis of GG-*g*-P(NIPAM-*co*-AA)/GO and evaluation of adsorption activity for the diclofenac and metformin

Bhagvan P. Kamaliya[1] · Pragnesh N. Dave[1] · Lakha V. Chopda[2]

Received: 15 October 2022 / Accepted: 22 May 2023 / Published online: 17 June 2023

Abstract

The grafting of biopolymer gum ghatti (GG) over the PNIPAM and PAA was done and loaded with graphene oxide (GO). Aim of this work is carried out combine adsorption of sodium diclofenac (SD) and metformin (MF) by the prepared hydrogels under influence of various parameters. The adsorbent GG-*g*-P(NIPAM-*co*-PAA)/GO(3 mg) chosen for adsorption activity as it displayed highest swelling capacity. The effect of amount of both adsorbents GG-*g*-P(NIPAM-*co*-PAA and GG-*g*-P(NIPAM-*co*-PAA)/GO(3 mg) showed that highest adsorption capacity found at 40 mg of adsorbents for both drugs at conditions: 100 mg/L concentration, 30 °C, 24 h and pH 6 and subsequently became stable. Both the drugs were removed in greater amount at 25 mg/L concentration, 24 h of contact time, 30 °C, 40 mg amount of both adsorbents and pH 6. Effect of time revealed that as time elevated from 2 h to 12 (100 mg/L concentration,, 30 °C, 40 mg amount of both adsorbents and pH 6) led to increase adsorption efficiency and after that increase time did not much impact on adsorption activity. Adsorption activity of hydrogels declined with increase of temperature (100 mg/L concentration, 12 h, 40 mg amount of both adsorbents and pH 6). The acidic conditions favored adsorption of SD while MF adsorbed under the weak acidic(100 mg/L concentration, 30 °C, 12 h, 40 mg amount of both adsorbents). However, basic conditions did not much influence on adsorption of MF but effected on adsorption activity of SD. Adsorption isotherm and kinetic model suggested that adsorption is homogenous and chemical in nature. The maximum adsorption capacity (q_m) found to be 289.01 and 154.55 mg/g for SD and MF respectively.

Highlights

- Synthesis of GG-*g*-P(NIPAM-*co*-AA)/GO
- Characterize by FT-IR, XRD, SEM and BET surface area
- The adsorption of sodium diclofenac and metformin was undertaken
- The hydrogel exhibited moderate and good adsorption activity for sodium diclofenac and metformin
- Adsorption process followed the Langmuir adsorption isotherm and pseudo-second kinetic model

Keywords Biopolymer · Grafting · Pollution · Adsorption · Green chemistry

Introduction

Water is the important and essential compound for surviving of creature life. It helps to regulate body temperature and other cell functions. In general, water assists to prevent urinary tract infections, kidney stones, and gallbladder deposit. The water pollution by the different kind of pollutants is the growing concern problem worldwide. The polluted water led to disturb the life of human being and other leaving organisms by causing life threatening diseases [1]. The high consumption of pharmaceuticals led to found in the water body as in the form of metabolites, neutral compound and conjugated complex and contributed to adverse effect on the human life and environment [2, 3]. Various classes of antibiotics such as β-lactams, tetracyclines, aminopenicillins and others are used to prevent infection caused by microorganism and used as s food additive in the livestock for promote the growth and weight gain [4]. Due to their low metabolism, they are ejected in the urine and

✉ Pragnesh N. Dave
pragnesh.dave@spuvvn.edu; pragnesh7@yahoo.com

[1] Department of Chemistry, Sardar Patel University, Vallabh Vidynagar, Gujarat 388 120, India

[2] B. N. Patel Institute of Paramedical & Science (Science Division), Sardar Patel Education Trust, Bhalej Road, Anand, Gujarat 370 001, India

feces in the unaltered form hence found in the aquatic environment and caused the harmful effect [5]. Diclofenac and metformin are frequently used to treat the inflammation and type 2 diabetes respectively. The different kind of toxicity of both has found, diclofenac caused several toxicities such as hepatoxicity, nephrotoxicit, neurotoxicity and reproductive toxicity [6]. Diclofenac contributed to oxidative stress by forming reactive oxygen species (ROS) [7]. Same as various toxicities have been caused by metformin also [8, 9]. To lessen the effect of both in the water system, some methods were commenced. For example, diclofenac and metformin were removed by 90% and 100% using advanced oxidation process [10]. The adsorbent (poly (AN-co-EGDMA-co-VBC) was able to remove 78% and 72% of diclofenac and metformin respectively [11]. A very few examples are available for the combine removal of diclofenac and metformin from aqueous system.

Hydrogel is the three dimensional peculiar network of cross-linked polymer that possessed the unique properties such high water adsorption capacity, softness, viscoelasticity etc. Presence of hydrophilic groups (-OH, -COOH, -$CONH_2$, -NH_2, SO_3H etc.) on the hydrogel contribute to swell it in the water. Due to its high swelling property in the water, it able to adsorb wide variety of impurities found in the water [12]. The biohydrogels gained significant interest especially biomedical engineering due to their biodegradability and biocompatibility [13, 14]. Hydrogel based biopolymer as adsorbent has been reported for the removal of pollutants. These included NaAlg-g-Poly(acrylic acid-co-acryl amide)/clinoptilolite hydrogel reported for the removal of a methylene blue(MB), poly(acrylamide-co-itaconic acid)/MWCNTs for the removal of Pb(II), xanthan gum-cl-poly(acrylic acid)/o-MWCNTs for the removal of MB and β-cylodextrin-*g*-PAAm for the removal of various organic pollutants and for the removal of hydrophobic micropollutants [15–18]. The gum ghatti is the natural non-starch polysaccharide gum obtained from the Anogeissus latifolia. The gum ghatti hydrogels devised for the removal of broad range of pollutants from the water system [19–22]. This work reports the synthesis of GG-*g*-P(NIPAM-*co*-AA)/GO for the combine removal of SD and MF. The GG biopolymer possessed unique carbohydrates that contained hydroxyl, carboxylic acid and amide functional groups [23–25] and further additional these functional groups and others attached to hydrogel after crosslinking with PNIPAM and AA and GO hence prepared hydrogels preferred for adsorption of SD and MF. The presence of functionality on SD and MF can be interacted with functionality of GG-*g*-P(NIPAM-*co*-AA)/GO hydrogel which ultimately resulted into adsorption of both drugs from the solution.

Experimental section

Materials

Gum ghatti (extra pure), acrylic acid (AA-98%), Ammonium persulfate (APS-98%), tetramethylethylenediamine-(TMED-99%) and N,N'- Methylenebisacrylamide (MBA-99%) were purchased from Loba Chemie (Mumbai, India). N-isopropylacrylamide (NIPAM-97%) was procured from TCI. Graphene oxide was purchased from Sigma Aldrich (Munich, Germany). Metformin hydrochloride (MF-99%) and sodium diclofenac (SD-99%) used in this study brought from HiMedia and Sigma Aldrich respectively.

Synthesis of Gum ghatti-g-poly (N-isopropylacrylamide-*cl*-acrylic acid)/GO

The hydrogel GG-*g*- P(NIPA-*co*-AA)/GO was prepared according to reported method [26–29]. The procedure involves - first, 0.5 g GG was added to 10mL of distilled water in a 100mL beaker. The dissolved solution was allowed to stir for 24 h for better dissolution of biopolymer and subsequently sonicated for 40 min of GO (1–5 mg), monomers NIPAM (0.2 g) and required amount of APS, TEMED and MBA as per shown in Table 1 were added to above solution. 1 mL of AA was furnished immediately to this solution. The whole solution heated at 50 °C for 3 h hot air oven. After 3 h, the beaker was allowed to cool at room temperature. The formed homo-polymer was extracted using consecutive acetone extraction. The hydrogel was allowed to dry gradually at 50 °C for 48 h and grounded into powder with a mortar and pestle. The composition of all materials was depicted in Table 1 and the reaction illustration is depicted in Fig. S1 and the Probable mechanism Scheme S1.

Table 1 Composition of prepared hydrogel

Sample id	GG (gm)	NIPAM (gm)	AA (mL)	APS (mg)	MBA (mg)	TEMED (mL)	GO (mg)	H_2O (ml)
GG-g-P(NIPAM-co-AA)	0.5	0.2	1.0	50	50	0.1	0	10
GG-g-P(NIPAM-co-AA)/GO	0.5	0.2	1.0	50	50	0.1	1	10
	0.5	0.2	1.0	50	50	0.1	2	10
	0.5	0.2	1.0	50	50	0.1	3	10
	0.5	0.2	1.0	50	50	0.1	4	10
	0.5	0.2	1.0	50	50	0.1	5	10

Characterization of hydrogel

Fourier transform infrared (FT-IR) spectra of materials recorded on Perkin Elmer Model using KBr plate method in the range of 400–4000 cm^{-1}. X-ray diffraction (XRD) of materials was carried out on Rigaku; miniflex 600, Japan with CuKα radiation ($\lambda = 1.5418$). Micromeritics, ASAP 2020 nitrogen adsorption-desorption analyzer used to determine the surface area and porosity of materials.

Swelling studies

The swelling capacities of different nanocomposite hydrogels were determined by soaking method. The weighted sample of nanohydrogel (100 mg) was soaked into clean distilled water for 24 h. The gained weight was measured after 24 h. The percentage of swelling was determined by Eq. 1.

Swelling was determined using equation presented in (1).

$$\text{Swelling} = \frac{W_s - W_d}{W_d} \times 100 \tag{1}$$

Where WS and Wd represent the dry and swollen masses of hydrogels respectively.

Stock solution preparation

The stock solution 1000 ppm (mg/L) of SD and MF was prepared by 1000 mg of SD and MF dissolved 1000 mL triple distilled water. For the better dissolution of solution, ultrasonication and stirring on magnetic stirrer was carried out. The solution was stored in refrigerator (4 °C) and used within 2 days. The required concentration for adsorption was diluted from the stock solution.

Adsorption study

The combine adsorption of SD and MF was carried out in batch mode by GG-*g*-P(NIPAM-*co*-AA)/GO hydrogels in 250mL standard sealed Erlenmeyer flasks containg 50mL solution of both drug [11, 30, 31]. The maximum λ_{max} of SD and MF was found to be 276 and 232.5 nm respectively which was recorded on UV- Vis double beam spectrophotometer (TCC-240 A, Shimadzu). The effect of amounts of both hydrogels was performed first. The 10–100 mg amount of both hydrogels was dispersed into 50 mL solution of 100 ppm of SD and MF at pH. The reaction tube was placed in shaker and stirred at 250 rpm and room temperature (rt) for 24 h. The adsorption capacity of hydrogels measured in changing the concentration of both drugs before and after adsorption. The adsorption capacity and removal efficiency was calculated by Eqs. 2 and 3 respectively.

$$qe = \frac{(C_0 - C_e) \times V}{m} \tag{2}$$

$$\text{Removal } \% = \frac{C_0 - C_e}{C_0} \times 100 \tag{3}$$

Here, C_0 and C_e presented the initial and at equilibrium concentrations (mg/L) of SD and MF respectively, *m* represents the weight of the adsorbent, V is the volume of the solution (L). The concentration of SD and MF was determined in mg/L. The effect of other parameters of SD and MF such variation in concentration(25–200 mg/L at room temperature and contact time 24 h), time (2–24 h at room temperature), temperature (20–60 °C at contact time 24 h) was done using 40 mg amount of adsorbents at pH 6. The experiment of effect of temperature was carried out on magnetic stirrer instead of shaker. The influence of pH (2–12) was conducted by employing 40 mg adsorbents amount at room temperature and 24 h contact time. The pH solution is adjusted by 1 M HCl and NaOH solution.

Adsorption isotherm

The four adsorption isotherms such as Langmuir Isotherm [17], Freundlich isotherm [17], Temkin Isotherm [32] and Dubinin–Kaganer–Radushkevich [17] were assessed for adoption phenomena. The detail equation of four adsorption isotherms are represented by following equations (4, 6, 7 and 8) respectively.

1. Langmuir Isotherm

$$\frac{C_e}{q_e} = \frac{1}{q_m K_L} + \frac{C_e}{q_m} \tag{4}$$

Ce is the equilibrium concentration of SD in the solution (mg/L), q_e is the adsorption capacity at equilibrium (mg/g), q_{max} is the maximum adsorption capacity (mg/g), and K_L Langmuir constant (L/mg).

The value of q_{max} and K_L defined from the slope and intercept from the plot of C_e/q_e against C_e, K_L is an important tool in the calculation of the dimensionless equilibrium parameters, R_L that explain the favorability of adsorption process, R_L is calculated from following equation

$$R_L = \frac{1}{1 + K_L C_0} \tag{5}$$

2. Freundlich isotherm

$$log\ q_e = log\ K_f + \frac{1}{n} log\ C_e \quad (6)$$

K_f is the Freundlich constant (mg/g), n is Freundlich exponent related to the adsorption intensity or surface heterogeneity (dimensionless). The values of isotherm constants (K_f and n) are defined from the intercept and slope of the linear plot of log q_e versus log C_e respectively.

3. Temkin Isotherm

$$q_e = BlnK_T + BlnC_e \quad (7)$$

B = is the heat of sorption constant, K_T is the binding constant K_T and B were determined by the from the slope and intercept of plot q_e against lnC_e

4. Dubinin–Kaganer–Radushkevich

$$lnq_e = lnq_m - \beta\ \varepsilon^2 \quad (8)$$

β (mol^2/kJ^2) is the constant related to the adsorption energy, q_m (mg/g) is the theoretical saturation capacity, Ɛ (kJ/mol) is the Polanyi potential q_m and β were calculated from the from the intercept and the slope of plot lnq_e against Ɛ^2, Ɛ and E (free energy of adsorption) calculated by following equations

$$\varepsilon = RT\ \ln(1 + \frac{1}{C_e}) \quad (9)$$

$$E = \frac{1}{\sqrt{2\beta}} \quad (10)$$

Kinetic studies

The three kinetic models such as Pseudo-1st -Order and 2nd Order Model [17] and Elovich model [17] were checked for the interaction between adsorbent and adsorbate which are shown by following equations (11, 12 and 13) respectively.

1. Pseudo-1st -Order Model and 2nd Order Models

$$\ln(q_e - q_t) = \ln q_e - K_1 t \quad (11)$$

$$\frac{t}{q_t} = \frac{1}{K_2 q_e^2} + \frac{t}{q_e}$$

q_e (mg/g) is the adsorption capacity at equilibrium; q_t (mg/g) is the adsorption capacity at time t;

k_1 (1/min) and k_2 (g/(mg.min)) are the first-order rate and the second-order rate constants,

The rate constants (k_1 and k_2) were determined from the slope and intercept of the plots of log ($q_e - q_t$) against t and t/qt against. t, respectively.

2. Elovich model

$$q_t = \frac{1}{\beta}\ln(\alpha\beta) + \frac{1}{\beta}\ln t \quad (12)$$

Where, q_t represents adsorption capacity at time *t*, β and α are the Elovich constants equivalent to the extent of surface coverage and rate of adsorption at zero coverage respectively.

3. Intraparticle diffusion model [33]

$$q_t = K_{IP} t^{\frac{1}{2}} + C_{IP} \quad (13)$$

Where, q_t presents adsorption capacity at time t, intercept C_{IP} reflects the boundary layer thickness effect and KIP indicates rate constants of intraparticle diffusion.

Results and discussion

Mechanism of formation of GG-*g*-P(NIPMA-*co*-AA)/GOand swelling property

Scheme S1 presents the detail mechanism of formation of GG-g-P(NIPMA-*co*-AA)/GO hydrogel [34]. TheSO4 $^{\bullet-}$ radical anions and OH$^{\bullet}$ radicals initiated the reaction (Initiation step). The active side on GG formed by these both reactive species (GG$^{\bullet}$). The formed GG$^{\bullet}$ propagated reaction by forming active side on NIPAM and AA that caused the grafting on GG. The crosslink agents end-up with formation of GG-g-P(NIPMA-*co*-AA) hydrogel. The measurement of swelling property is shown in the Table 2. It showed that swelling property of GG-*g*-*P*(NIPAM-*co*-AA) (GNAGO-0) enhanced as loading of GO increased from 1 mg to 3 mg

Table 2 Measurement of swelling property of hydrogel

Sample id	Swelling (g/g)
GG-g-P(NIPAM-co-AA)-GNAGO-0	3.14
GG-g-P(NIPAM-co-AA)/GO (1 mg)- GNAGO-1	3.07
GG-g-P(NIPAM-co-AA)/GO (2 mg)- GNAGO-2	3.15
GG-g-P(NIPAM-co-AA)/GO (3 mg)- GNAGO-3	3.43
GG-g-P(NIPAM-co-AA)/GO (4 mg)- GNAGO-4	3.15
GG-g-P(NIPAM-co-AA)/GO (5 mg)- GNAGO-5	2.95

then after decreased. The 3 mg loading of GO exhibited high swelling efficiency hence it was chosen for adsorption of SD and MF.

Swelling studies

The measurement of swelling property of hydrogels is shown in the Table 2. It showed that increased the amount of GO from 1 to 3 mg led to enhance the swelling property and then after it decreased as amount increased from 4 to 5 mg. The 3 mg of GO over to GG-*g*-P(NIPMA-*co*-AA) exhibited highest water holding capacity hence it preferred for combine adsorption of SD and MF.

FT-IR analysis

The FT-IR spectra of GG, GO, GG-*g*-*P*(NIPAM-*co*-AA) (GNAGO-0) and GG-*g*-*P*(NIPAM-*co*-AA) (GNAGO-3) is shown in the Fig. 1. The FT-IR spectra of GG confirmed about feature functional groups presence in GG. The bands at 3340 cm^{-1} (broad peak) and 2934 cm^{-1} corresponded to stretching vibration of O-H and C-H respectively [22, 35]. The band visualized at 1004 cm^{-1} ascribed of strong vibration of C-O and band at 541 cm^{-1} (low intense) assigned to bending vibration of C-O or O-H functionality [22, 36]. The strong band found at 1710 cm^{-1} revealed of stretching vibration of C = O group of carboxylic acid group of AA present in GG-*g*-*P*(NIPAM-*co*-AA)(GNAGO-0) [37]. The stretching vibration of N-H of amide functional group of PNIPAM attributed at 1600 cm^{-1} (low intense band) [37–39]. The band at 3750 cm^{-1}can be assigned to stretching vibration of hydroxyl functional group of carboxylic acid of AA. The FT-IR spectra of GO showed that required functionality found in the GO [40]. The FT-IR spectra of GG-*g*-*P*(NIPAM-*co*-AA) indicated that after loading of GO did not alter the spectra of GG-*g*-*P*(NIPAM-*co*-AA). The special bands of GO did not evaluate in the GG-*g*-Poly (NIPAM-*co*-AA) which is the signing of homogeneous dispersion of GO over to GG-*g*-*P*(NIPAM-*co*-AA).

XRD analysis

The Fig. 2 depicted the XRD of GG, GG-*g*-*P*(NIPAM-*co*-AA)(GNAGO-0) and GG-*g*-*P*(NIPAM-*co*-AA))/GO) (GNAGO-1).The peak at $2\theta = 18.7°$ is the characteristic peak of GG and shifted to higher angle after grafting of NIPAM and PAA to GG [41]. The same observation found in the case of grafting of PAA over to GG. In this case, after grafting of PAA to GG caused to slightly shifted peak at higher angle [42]. After loading of GO, this was more shifted to higher angle. In the case of GG-*g*-*P*(NIPAM-*co*-AA))/GO)(GNAGO-1), it shifted from 18.7° to 20.42° while loading of GO to GG-*g*-P(NIPAM-*co*-AA)(GNAGO-0) caused to shifted peak at slightly higher range (20.7°). It has been observed that this peak became less broad compared to GG as grafting of PNIPAM and PAA and loading of GO. It showed that successfully formation of GG-*g*-P(NIPAM-*co*-AA)(GNAGO-0) hydrogel and loading of GO to GG-*g*-P(NIPAM-*co*-AA)(GNAGO-0).

SEM images of hydrogel study

SEM images of pure GO, GG-*g*-*P*(NIPAM-*co*-AA) (GNAGO-0) and GG-*g*-*P*(NIPAM-*co*-AA))/GO) (GNAGO-1) have been shown in the Fig. 3. The Fig. 3a shows that GO possessed multi-layered, disordered structure, as well as a pleated sheet-like structure [43]. The surface morphology of the hydrogel without graphene

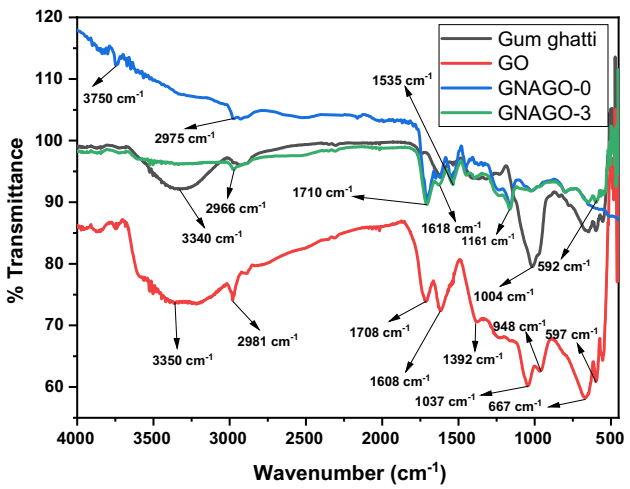

Fig. 1 FT-IR of GG, GNAGO-0 and GNAGO-3

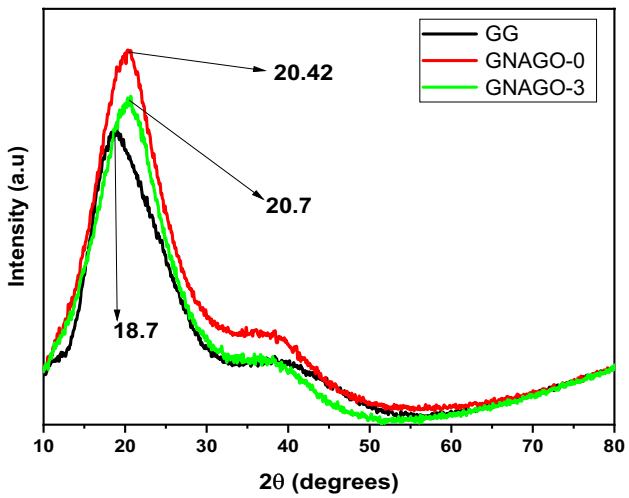

Fig. 2 XRD of GG, GNAGO-0 and GNAGO-3

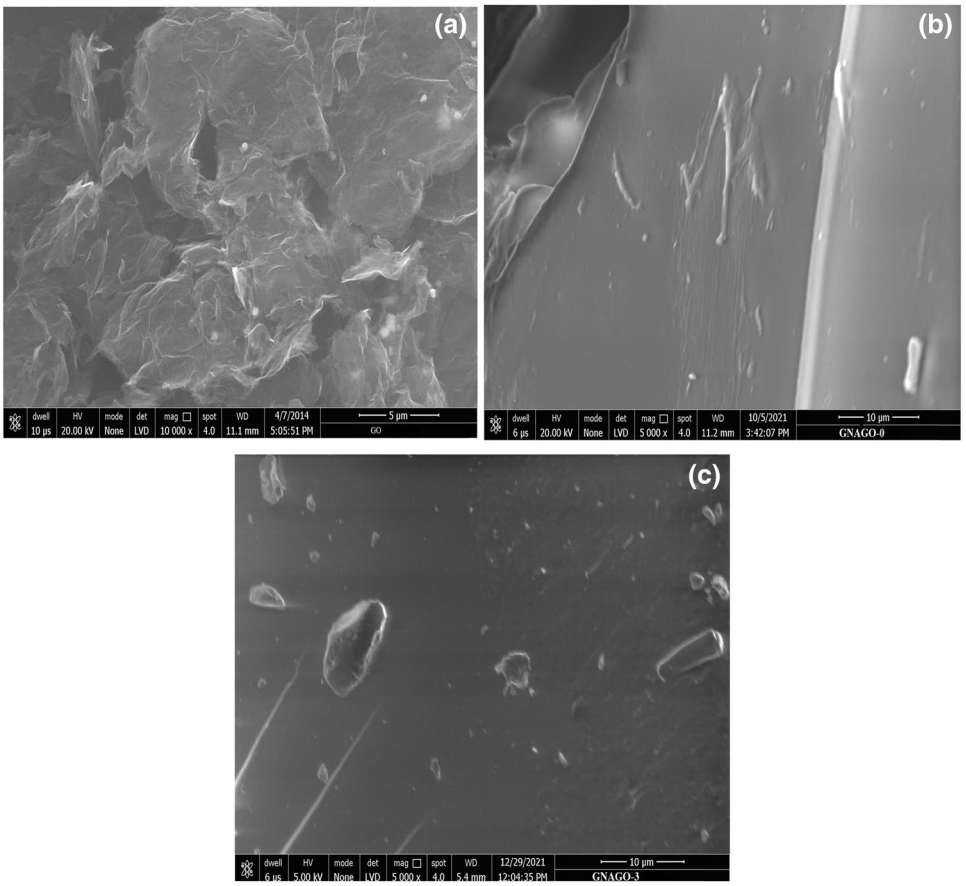

Fig. 3 FE-SEM images for **a** pure graphene oxide, **b** GNAGO-0 hydrogel and **c** GNAGO-3 hydrogel

oxide found to be rough but it became smooth after loading of graphene oxide.

Brunauer-Emmett-Teller (BET) surface area

The BET theory used to understand adsorption of molecule on the surface of solid. It provided the information

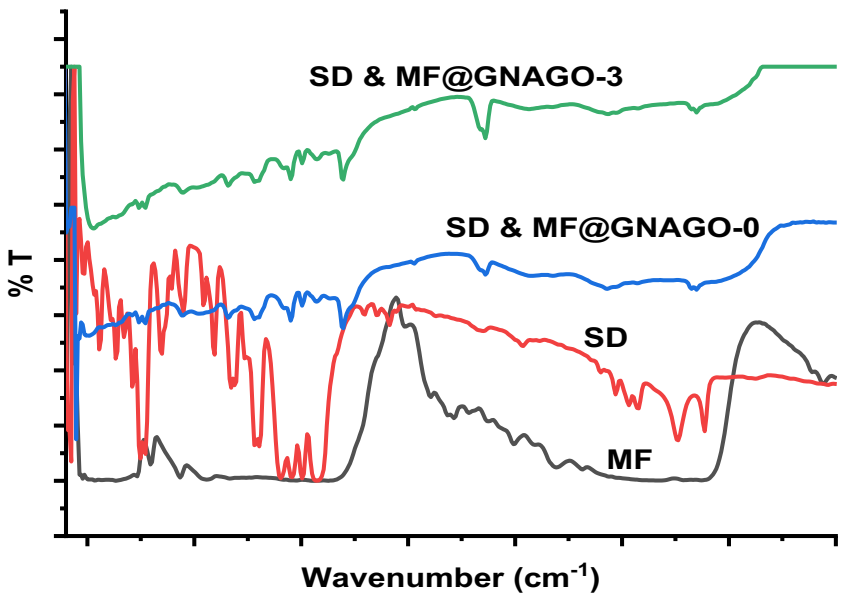

Fig. 4 FT-IR of SD and MF before and after adsorption

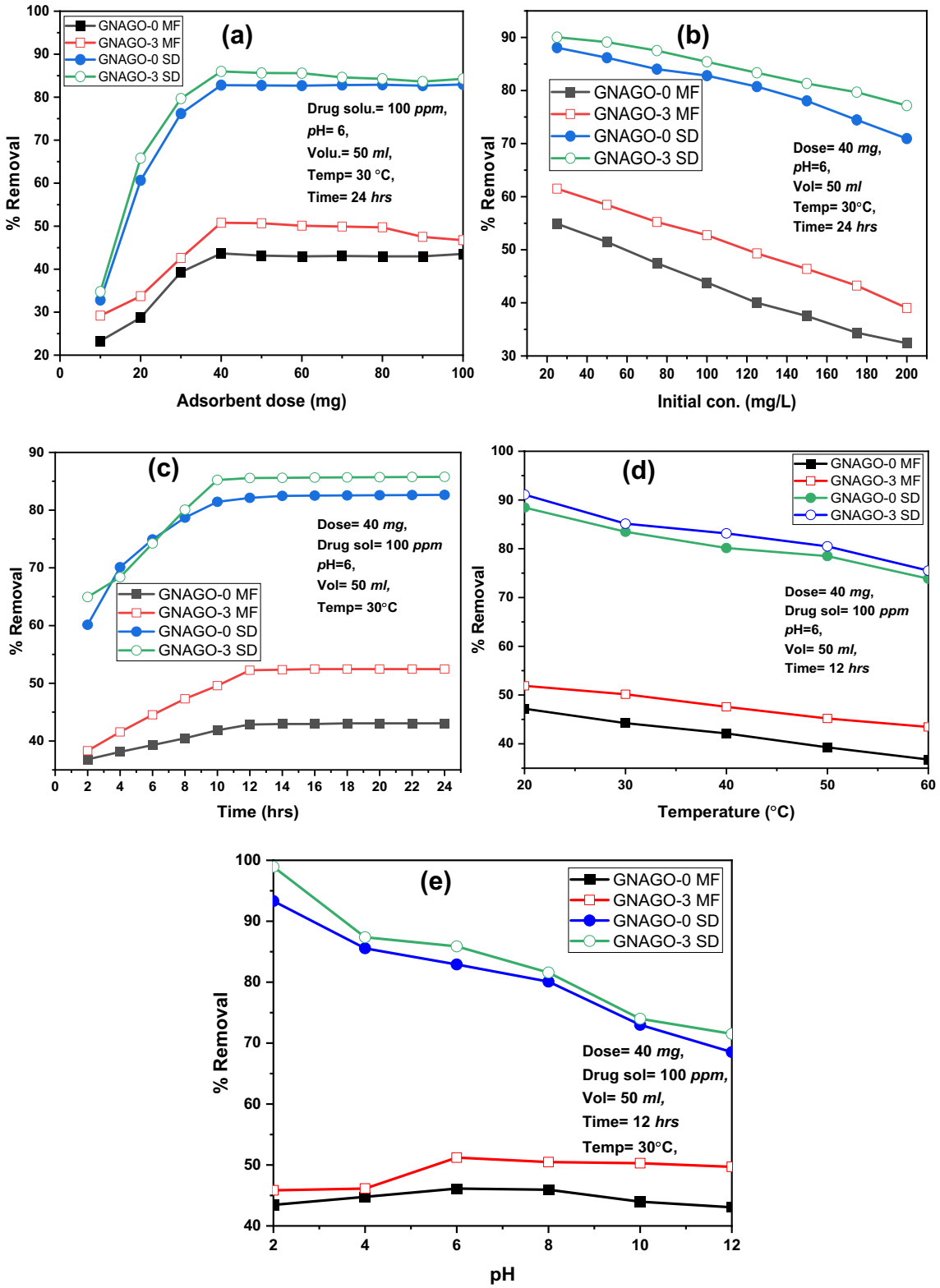

Fig. 5 Removal efficiency of adsorbents: **a** Effect of amount **b** Effect of concentration **c** Effect of time **d** Effect of temperature **e** Effect of pH

of the effects of GO on the surface area and pore volume of the polymer matrix of GG-g-P(NIPAM-co-AA) [31]. The BET surface area, pore volume, and pore diameter of GG-g-P(NIPAM-co-AA) were estimated to 0.1785m^2/g, 0.001314cm^3/g, and 294.42Å, respectively and these values were increased to 0.3031 m^2/g, 0.002792 cm^3/g, and 932.45 Å respectively by incorporation of 3 mg of GO in the polymer matrix.

Adsorption activity

The FT-IR of SD and MF (Fig. 4) before and after adsorption showed that SD and MF adsorbed over the hydrogels. The adsorption study of SD and MF indicated that as the amount of both adsorbents GG-*g*-P(NIPAM-*co*-AA)–GNAGO-0 and GG-*g*-P(NIPAM-*co*-AA)/GO(3 mg)-GNAGO-3 increased led enhance the removal efficiency as shown in the Fig. 5a and Table S1. The 40 mg of adsorbents showed highest removal efficiency. The adsorbents GNAGO-0 and GNAGO-3 displayed 43.64% and 50.77% removal efficiency for MF while for SD, they showed 82.78% and 85.99% removal efficiency. The loading of GO enhanced the removal efficiency. The removal efficiency became almost stable as the loading of adsorbents enhanced from 40 mg. The concentration of both adsorbents increased led to decrease the removal efficiency (Fig. 5b and Table S2). The 25 mg/L found to be best concentration where highest removal efficiency has been achieved. The influence of time revealed that as the time increase from 2 to 12 h, removal efficiency increased and further increase in time did not much effect on the removal efficiency (Fig. 5c and Table S3). The increase temperature showed that as the temperature increased led to decrease the removal efficiency. The highest removal efficiency found at 20 °C (Fig. 5d and Table S4). The effect of pH on removal efficiency indicated that as pH increased from 2 to 6, removal efficiency of MF elevated and little bit decrease as the pH increases from 6 to 12(Fig. 5e and Table S5). The removal efficiency of SD drastically decreased as the pH of solution increased from 2 to 12(Fig. 5e and Table S5). The enhance pH caused to decrease the removal efficiency of SD and did not much change for MF indicated that as pH of solution increased, surface charge of adsorbent could be negative charge and could became positive charge as the pH decreased. The presence of hydroxyl and carboxylic acid functional groups on GG-*g*-P(NIPAM-*co*-AA)/GO easily underwent protonation in acidic pH and convert adsorbent surface into positive charge while reverse trend can observe at high pH. At acidic pH, positive surface charge of adsorbent interacted well with negative charge of SD. and caused to increase the removal efficiency but high acidic and basic conditions disfavored adsorption of MF because of at these conditions concentration of positive and negative charge can be increase on adsorbents and MF which can repel each other (adsorbents and MF) which can be contribute to low removal efficiency of MF under high acidic and basic conditions. Highest adsorption of MF.

found at pH 6 where MF can bear positive charge and adsorbents can have negative charge or vice versa. The reversed trend obtained in the case of xanthan gum-*g*-PAA/oxidize MWCNT [16]. In this case increased pH led to increase the removal efficiency of MB. The increased pH ionize carboxylic acid group of adsorbent into carboxylate ion which interacted more with cationic MB dye. Based on above argument, adsorption proceeded through electrostatic interaction.

Adsorption isotherm

The adsorption process of contaminants over the surface of adsorbent explains by the isotherms. The adsorption isotherms describe the how the adsorbent interacts with adsorption site of adsorbate. Various adsorption isotherms were assessed for this one. The four adsorption models are shown in Fig. 6. such as Langmuir, Freundlich, Temkin and Dubinin–Kaganer–Radushkevich (DKR) were undertook for the understanding the interaction mechanism. The results obtained from the adsorption isotherms indicated that adsorption followed the Langmuir adsorption isotherm model for SD and MF. It indicates that nature of interaction is monolayer and homogeneous [44]. The various parameters from the Langmuir adsorption isotherms such asq_e(adsorption capacity-mg/g) at equilibrium, K_L(Langmuir constant –L/mg) and R_L (separation factor) were determined as shown in the Tables S6 to S7. The value of R_L suggested that favorable adsorption of SD and MF over the surface of adsorbent [17]. The value of 1/*n*(relates to adsorption intensity or surface heterogeneity) shows chemisorption [45]. The value of free energy (E) of adsorption calculated by DKR isotherm reflects that adsorption proceeds through strong chemisorption [46].

Kinetics and thermodynamic studies

Kinetic model provides the information about adsorption rate, and sorption mechanism that involved mass transfer, diffusion and reaction on the adsorbent surface. The four kinetic models were also assessed. Various kinetic parameters were determined as shown in Fig. 7. (Tables S8 and S9). The SD and MF followed the pseudo-second–order model which also suggested about the chemisorption. The intra-particle diffusion model suggested that adsorption occurred in the two stages [33]. The first stage involves surface adsorption and second stage contains

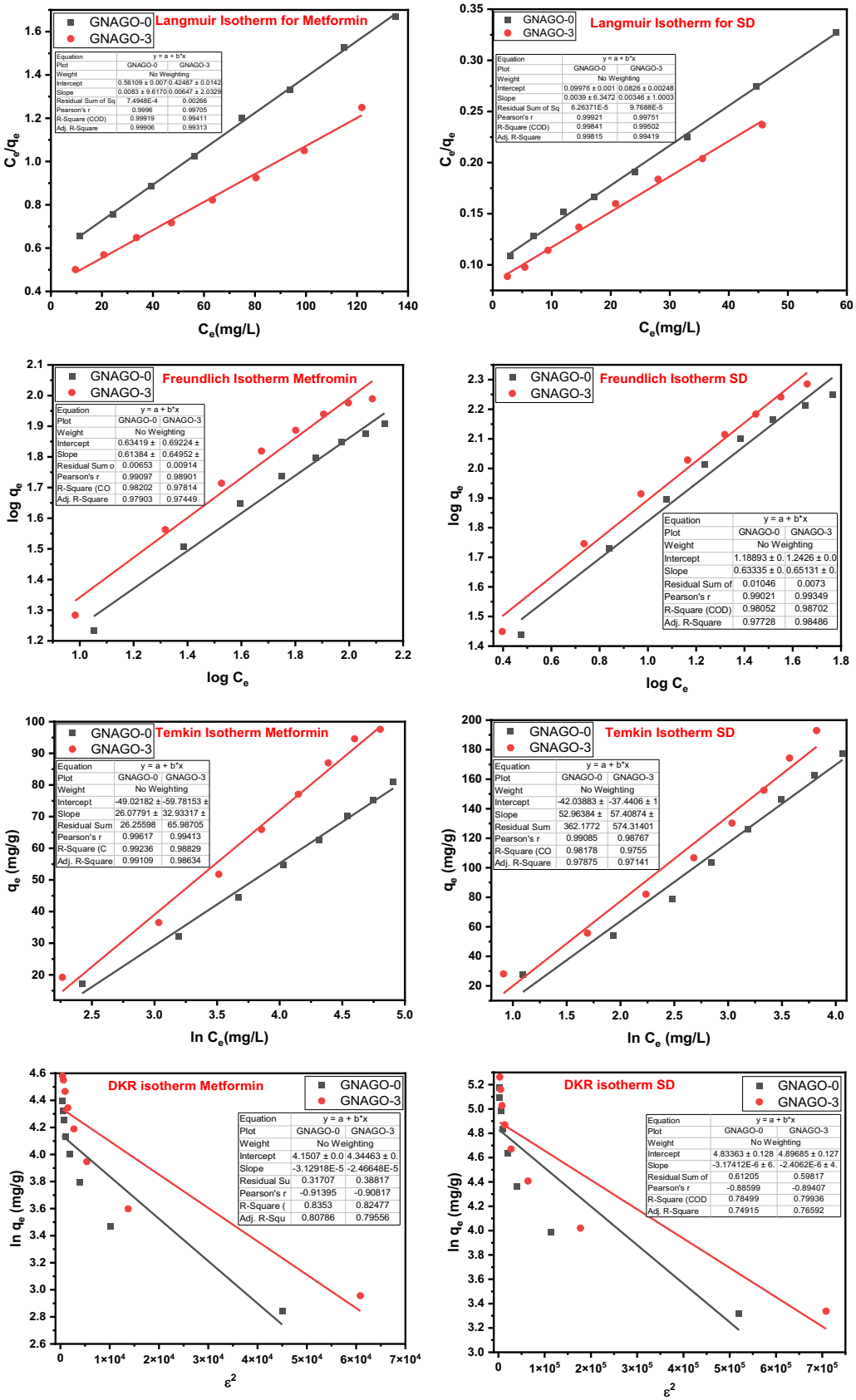

Fig. 6 Adsorption isotherms

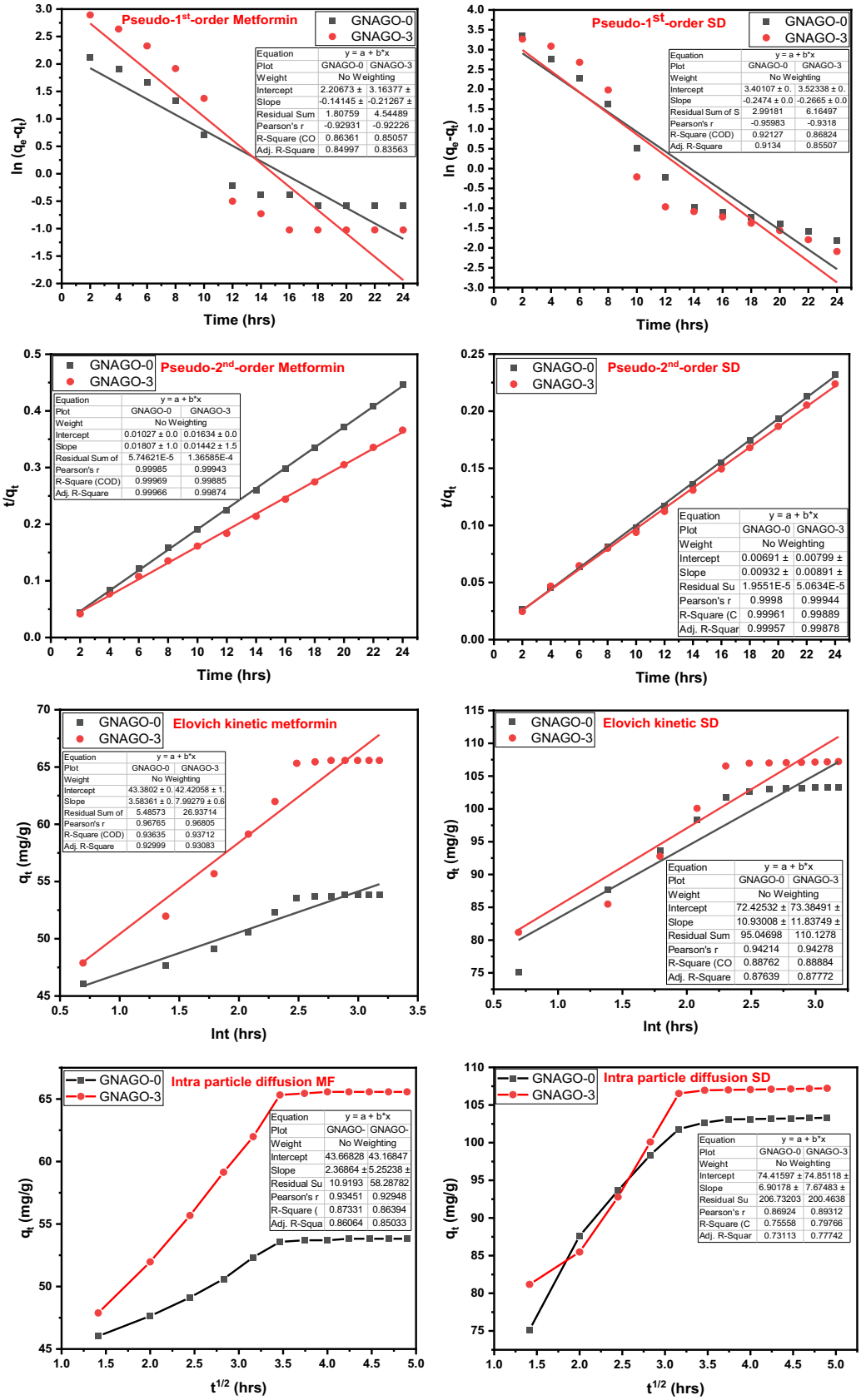

Fig. 7 Kinetic models of adsorbents

Table 3 Comparison of maximum q_e of various adsorbents for MF and SD

S.No	Adsorbent	Adsorption capacity(mg/g)	Reference
	Metformin removal		
1	Gg-cl-poly(NIPA-co-AA)/$CoFe_2O_4$	151.057	[31]
2	Graphene Oxide nanoparticles	122.61	[47]
3	Graphene Oxide	96. 748	[48]
4	HXL poly(AN-co-EGDMAco-VBC) (combine adsorption)	61.0 (diclofenac) 5.1 (metformin)	[11]
5	GG-g-P(NIPAM-co-AA)/GO	154.56	Present work
	Sodium diclofenac		
7	PAA/poly(ethylene imine)	32.42	[49]
8	Chitosan/magnetic composite	196	[50]
9	(SA/CNC/PVA)@PE	418.41	[51]
10	GG-g-PAA/-O-MWCNT	229.36	[52]
11	GG-g-P(NIPAM-co-AA)/GO	289.01	Present work

intra-particle diffusion. Based on the evaluated kinetic models, adsorption of MF followed the sequence order: Pseudo second order > Elovich > intra-particle diffusion > Pseudo first order while SD followed order: Pseudo second order > Elovich > > Pseudo first order > intra-particle diffusion. The thermodynamic parameters was also investigated (Figs. S2, S3, Tables S10 and S11) and value of ΔH° and ΔG°(KJ/mol) indicates that adsorption is exothermic and spontaneous in nature.

Comparison of adsorption capacity

The adsorption capacity of combine adoration of SD and MF was compared with individual adsorption capacity of SD and MF reported in literature was presented in the Table 3. It shows that hydrogel GG-*g*-P(NIPAM-*co*-AA)/GO exhibited high adsorption capacity towards combine adsorption of SD and MF.

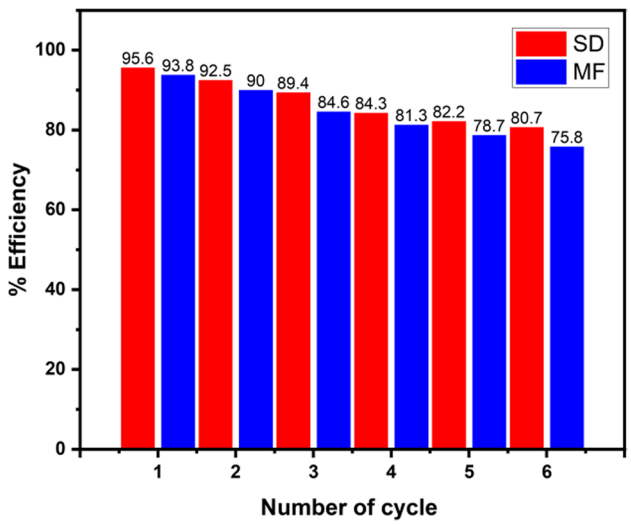

Fig. 8 Reusability study of Gum ghatti-*cl-poly*(NIPA-*co*-AA)/GO hydrogel for the removal of SD and MF

Regeneration and reusability studies

The reusability of the adsorbent is a significant factor for estimating the cost-effective applicability and satisfying the ecological and economic thresholds. Sodium diclofenac and metformin adsorption onto Gum ghatti-cl-poly(NIPA-co-AA)/GO was carried out at SD and MF concentration (100 mg/L). To further examine the reusability, the experiments were reiterated (up to Six times) by exposing a reacted GNAGO to a fresh SD and MF solution. Each time following the reaction, the GNAGO was collected from the solution by filtrate and washed with ethanol and 0.02 N NaOH solution and dried in the oven at 50 °C before being used for the next adsorption recycle.

The optimized conditions were followed for this experiment. Results are presented in Fig. 8 The adsorption percentage decreased SD from 95.6% in the first cycle to 80.7% in the sixth cycle and MF from 93.8% in the first cycle to 75.8% in the sixth cycle. This decrease in adsorption percentage may be due to the entrapment of SD and MF molecules onto the hydrogel surface that reduced the adsorption. Therefore, it could be concluded that GNAGO could be considered an economical adsorbent. The decrease of specific surface area and functional groups might contribute to the lower adsorption capacity of SD and MF onto GNAGO.

Conclusions

The hydrogel GG-*g*-P(NIPAM-*co*-AA)/GO was prepared by free radical polymerization using APS initiator which cross-linked by the cross-linking agents and loaded by GO during the polymerization. FT-IR and XRD were used to characterize the GG-*g*-P(NIPAM-*co*-AA)/GO hydrogel. The hydrogel GG-*g*-P(NIPAM-*co*-AA)/GO (3 mg) was preferred for combine adsorption of SD and MF as it exhibited high swelling property. Both techniques revealed that NIPAM and AA were grafted over to GG. Incorporation of GO over to GG-*g*-P(NIPAM-*co*-AA) improved the adsorption of drugs. The effect of various parameters over combine adsorption of drugs indicated that SD adsorbed more than MF. The high adsorption of SD can attribute to presence of carboxylic acid group of SD which efficiently interacted with hydroxyl group of GG. The effect of pH showed that acidic condition favored the adsorption of SD over to MF and adsorption of MF enhanced under the mild acidic condition. The adsorption of SD and MF followed the Langmuir adsorption isotherm, Pseudo second order kinetics models and thermodynamic study indicated adsorption of SD and MF over hydrogel surface is monolayer ,adsorption process is chemisorption and spontaneous in nature.

Supplementary information The online version contains supplementary material available at https://doi.org/10.1007/s40201-023-00867-w.

Acknowledgements The authors acknowledge Department of Chemistry, Physics and CISST of SPU and SICART of V.V. Nagar to utilize their characterization facility.

Author contributions Pragnesh N Dave has Conceptualized the research problem, review and editing of manuscript, Lakha V Chopda has contributed in in writing draft of manuscript original draft, Bhagvan Kamaliya contributed in methodology, formal analysis. All authors contributed to the study conception and design. Data collection and analysis were performed by Bhagvan Kamaliya and Lakha V Chopda. The first draft of the manuscript was written by Lakha V Chopda and Pragnesh N Dave had critically revised the final manuscript. and all authors commented on previous versions of the manuscript. All authors read and approved the final manuscript.

Data availability Not applicable for that specific section.

Declarations

The authors declare that no funds, grants, or other support were received during the preparation of this manuscript.

Research data policy All data generated or analysed during this study are included in this published article.

Ethical statement The research involving no human participants, their data or biological material.

Competing interests Authors disclose no financial or non-financial interests that are directly or indirectly related to the work submitted for publication.

References

1. Amin MT, Alazba AA, Manzoor U. A review of removal of pollutants from water/wastewater using different types of nanomaterials. Adv Mater Sci Eng. 2014;2014:1–24.
2. ChanderV, Sharma B, Negi V, Aswal RS, Singh P, Singh R, et al. Pharmaceuticalcompounds in drinking water. J Xenobiot. 2016;6.
3. Patel M, Kumar R, Kishor K, Mlsna T, Pittman CU, Mohan D. Pharmaceuticals of emerging concern in aquatic systems: chemistry, occurrence, effects, and removal methods. Chem Rev Am Chem Soc. 2019;119:3510–673.
4. Damiri F, Dobaradaran S, Hashemi S,Foroutan R, Vosoughi M, Sahebi S, et al. Waste sludge from shipping docks as acatalyst to remove amoxicillin in water with hydrogen peroxide and ultrasound.Ultrason Sonochem. 2020;68:105187.
5. BergamontiL, Bergonzi C, Graiff C, Lottici PP, Bettini R, Elviri L. 3D printed chitosanscaffolds: A new TiO2 support for the photocatalytic degradation of amoxicillinin water. Water Res. 2019;163:114841.
6. Adeyemi WJ, Omoniyi JA, Olayiwola A, Ibrahim M, Ogunyemi O, Olayaki LA. Elevated reproductive toxicity effects of diclofenac after withdrawal: investigation of the therapeutic role of melatonin. Toxicol Rep Elsevier Inc. 2019;6:571–7.
7. Tella T, Adegbegi A, Emeninwa C, Odola A, Ayangbenro A, Adaramoye O. Evaluation of the antioxidative potential of diisopropyldithiocarbamates sodium salt on diclofenac-induced toxicity in male albino rats. Toxicol Rep Elsevier. 2022;9:828–33.
8. Leonaviciute D, Madsen B, Schmedes A, Buus NH, Rasmussen BS. Severe metformin poisoning successfully treated with simultaneous Venovenous Hemofiltration and prolonged intermittent hemodialysis. Case Rep Crit Care Hindawi Limited. 2018;2018:1–4.
9. Wang GS, Hoyte C. Review of Biguanide (Metformin) toxicity. J Intensive Care Med. 2019;34:863–76. SAGE Publications Inc.
10. Maćerak AL, Kerkez Đ, Bečelić-Tomin M, Pilipović DT, Kulić A, Jokić J, et al. Removal of diclofenac and metformin from water in laboratory photo reactor. Environment,Green Technology, and Engineering International Conference. Basel Switzerland: MDPI A. 2018;1288.
11. Shaipulizan NS, Jamil SNAM, Abdullah LC, Choong TSY, Kamaruzaman S, Subri NNS, et al. Hypercrosslinked poly(AN-co-EGDMA-co-VBC): synthesis via suspension polymerization, characterizations, and potential to adsorb diclofenac and metformin from aqueous solution. Colloid Polym Sci Springer Sci Bus Media Deutschland GmbH. 2020;298:1649–67.
12. Ahmed EM, Hydrogel. Preparation, characterization, and applications: a review. J Adv Res. 2015;6:105–21. Elsevier B.V.
13. Min JH, Patel M, Koh WG. Incorporation of conductive materials into hydrogels for tissue engineering applications. Polym (Basel). 2018;10:1–36.
14. Dubey N, Kushwaha CS, Shukla SK. A review on electrically conducting polymer bionanocomposites for biomedical and other applications. Int J Polym Mater Polym Biomater Taylor Francis Inc. 2020;69:709–27.
15. Rashidzadeh A, Olad A, Salari D. The effective removal of methylene blue dye from aqueous solutions by NaAlg-g-poly(acrylic acid-co-acryl amide)/clinoptilolite hydrogel nanocomposite. Fibers Polym Korean Fiber Soc. 2015;16:354–62.
16. Makhado E, Pandey S, Nomngongo PN, Ramontja J. Preparation and characterization of xanthan gum-cl-poly(acrylic acid)/o-MWCNTs hydrogel nanocomposite as highly effective re-usable adsorbent for removal of methylene blue from aqueous solutions. J Colloid Interface Sci Acad Press Inc. 2018;513:700–14.
17. Mohammadinezhad A, Marandi GB, Farsadrooh M, Javadian H. Synthesis of poly(acrylamide-co-itaconic acid)/MWCNTs

superabsorbent hydrogel nanocomposite by ultrasound-assisted technique: swelling behavior and pb (II) adsorption capacity. Ultrason Sonochem Elsevier B V. 2018;49:1–12.
18. Song X, Mensah NN, Wen Y, Zhu J, Zhang Z, Tan WS, et al. β-Cyclodextrin-polyacrylamide hydrogel for removal of organic micropollutants from water. Molecules MDPI AG. 2021;26:5031.
19. Mittal H, Mishra SB. Gum ghatti and Fe3O4 magnetic nanoparticles based nanocomposites for the effective adsorption of rhodamine B. Carbohydr Polym. 2014;101:1255–64.
20. Mittal H, Kumar V, Alhassan SM, Ray SS. Modification of gum ghatti via grafting with acrylamide and analysis of its flocculation, adsorption, and biodegradation properties. Int J Biol Macromol. 2018;114:283–94 (Elsevier B.V).
21. Mondal H, Karmakar M, Dutta A, Mahapatra M, Deb M, Mitra M, et al. Tetrapolymer Network Hydrogels via Gum Ghatti-Grafted and N-H/C-H-Activated allocation of monomers for composition-dependent superadsorption of metal ions. ACS Omega Am Chem Soc. 2018;3:10692–708.
22. Puri V, Sharma A, Kumar P, Singh I, Huanbutta K. Synthesis and characterization of Thiolated Gum Ghatti as a Novel Excipient: development of compression-coated mucoadhesive tablets of domperidone. ACS Omega Am Chem Soc. 2021;6:15844–54.
23. Deshmukh AS, Setty CM, Badiger AM, Muralikrishna KS. Gum ghatti: a promising polysaccharide for pharmaceutical applications. Carbohydr Polym. 2012;87:980–6.
24. Sharma K, Kaith BS, Kalia S. Gum ghatti-based biodegradable and conductive carriers for colon-specific drug delivery. Colloid-Polym Sci. 2015;293:1181–90.
25. Sharma K, Virk K, Kumar V, Sharma SK, Sharma V. Preparation and characterizations graft copolymer of poly(acrylamide-aniline)-grafted Gum ghatti [Internet]. Mater Today Proc. 2020. Available from: www.sciencedirect.comwww.materialstoday.com/proceedings2214-7853.
26. Liu R, Liang S, Tang XZ, Yan D, Li X, Yu ZZ. Tough and highly stretchable graphene oxide/polyacrylamide nanocomposite hydrogels. J Mater Chem. 2012;22:14160–7.
27. Li B, Wu C, Wang C, Luo Z, Cao J. Fabrication of tough, self-recoverable, and electrically conductive hydrogels by *in situ* reduction of poly(acrylic acid) grafted graphene oxide in polyacrylamide hydrogel matrix. J ApplPolym Sci. 2020;137:48781. John Wiley and Sons Inc.
28. Sharma B, Thakur S, Trache D, Nezhad HY, Thakur VK. Microwave-assisted rapid synthesis of reduced graphene oxide-based gum tragacanth hydrogel nanocomposite for heavy metal ions adsorption. Nanomater MDPI AG. 2020;10:1–22.
29. Karunarathna MHJS, Bailey KM, Ash BL, Matson PG, Wildschutte H, Davis TW, et al. Nutrient capture from aqueous waste and photocontrolled fertilizer delivery to tomato plants using fe(III)-polysaccharide hydrogels. ACS Omega Am Chem Soc. 2020;5:23009–20.
30. Dave PN, Chopda LV, Kamaliya BP. Synthesis of a Polyacrylic-Grafted, Multiwalled Carbon Nanotube-Loaded Gum Ghatti Hydrogel for Diclofenac Removal. Chem Eng Technol [Internet]. 2023; Available from: https://onlinelibrary.wiley.com/doi/10.1002/ceat.202200367.
31. Dave PN, Kamaliya B, Macwan PM, Trivedi JH. Fabrication and characterization of a gum ghatti-cl-poly(N-isopropyl acrylamide-co-acrylic acid)/CoFe2O4 nanocomposite hydrogel for metformin hydrochloride drug removal from aqueous solution. Curr Res Green Sustain Chem. 2023;6:100349. Elsevier B.V.
32. Sharma G, Sharma S, Kumar A, Naushad M, Du B, Ahamad T et al. Honeycomb structured activated carbon synthesized from Pinus roxburghii cone as effective bioadsorbent for toxic malachite green dye. J Water Process Eng. 2019;32:100931. Elsevier Ltd.
33. Riahi K, Chaabane S, Thayer B, Ben. A kinetic modeling study of phosphate adsorption onto phoenix dactylifera L. date palm fibers in batch mode. J Saudi Chem Soc Elsevier B V. 2017;21:143–52.
34. Sharma K, Kaith BS, Kumar V, Kumar V, Som S, Kalia S, et al. Synthesis and properties of poly(acrylamide-aniline)-grafted gum ghatti based nanospikes. RSC Adv. 2013;3:25830–9.
35. Kaith BS, Sharma K, Kumar V, Kalia S, Swart HC. Fabrication and characterization of gum ghatti-polymethacrylic acid based electrically conductive hydrogels. Synth Met. 2014;187:61–7.
36. Sharma K, Kumar V, Kaith BS, Som S, Kumar V, Pandey A, et al. Synthesis of biodegradable gum ghatti based poly(methacrylic acid-aniline) conducting IPN hydrogel for controlled release of amoxicillin trihydrate. Ind Eng Chem Res Am Chem Soc. 2015;54:1982–91.
37. Ma T, Li X, Zhao D, Qiu G, Shi X, Lu X. A novel method to in situ synthesis of magnetic poly(N-isopropylacrylamide-co-acrylic acid) nanogels. Colloid Polym Sci Springer Verlag. 2016;294:1251–7.
38. Zhang M, Li Y, Yang Q, Huang L, Chen L, Ni Y, et al. Temperature and pH responsive cellulose filament/poly (NIPAM-co-AAc) hybrids as novel adsorbent towards pb(II) removal. Carbohydr Polym. 2018;195:495–504 (Elsevier Ltd).
39. Park Y, Hwang M, Kim M, Park E, Noda I, Jung YM. Characterization of the phase transition mechanism of P(NiPAAm-co-AAc) copolymer hydrogel using 2D correlation IR spectroscopy. Spectrochim Acta A Mol Biomol Spectrosc. 2021;252:119525. Elsevier B.V.
40. Çiplak Z, Yildiz N, Cąlimli A. Investigation of graphene/Ag nanocomposites synthesis parameters for two different synthesis methods. Fullerenes nanotubes and carbon nanostructures. Bellwether Publishing Ltd. 2015;23:361–70.
41. Pal P, Singh SK, Mishra S, Pandey JP, Sen G. Gum ghatti based hydrogel: microwave synthesis, characterization, 5-Fluorouracil encapsulation and 'in vitro' drug release evaluation. Carbohydr Polym. 2019;222. Elsevier Ltd.
42. Sharma K, Kumar V, Chaudhary B, Kaith BS, Kalia S, Swart HC. Application of biodegradable superabsorbent hydrogel composite based on gum ghatti-co-poly(acrylic acid-aniline) for controlled drug delivery. Polym Degrad Stab Elsevier Ltd. 2016;124:101–11.
43. E JSC, Gopi S, A R, Pius GS. Highly crosslinked 3-D hydrogels based on graphene oxide for enhanced remediation of multi contaminant wastewater. J Water Process Eng Elsevier. 2019;31:100850.
44. Avcu T, Üner O, Geçgel Ü. Adsorptive removal of diclofenac sodium from aqueous solution onto sycamore ball activated carbon – isotherms, kinetics, and thermodynamic study. Surf Interfaces. 2021;24:101097. Elsevier B.V.
45. Sadik WAA, El-Demerdash AGM, Abbas R, Gabre HA. Fast synthesis of an eco-friendly starch-grafted poly(N,N-dimethyl acrylamide) hydrogel for the removal of acid red 8 dye from aqueous solutions. Polym Bull Springer. 2020;77:4445–68.
46. Kadhim ZN. Using of isolated hydroxyapatite from sheep bones to remove lead (II) from aqueous solution and studying the thermodynamics and adsorption isotherm. Asian J Appl Sci [Internet] 2016;2321–0893. Available from:www.ajouronline.com.
47. Balasubramani K, Sivarajasekar N, Naushad M. Effective adsorption of antidiabetic pharmaceutical (metformin) from aqueous medium using graphene oxide nanoparticles: equilibrium and statistical modelling. J Mol Liq [Internet]. 2020;301:112426. https://doi.org/10.1016/j.molliq.2019.112426. (Elsevier B.V.).
48. Zhu S, Liu Y-g, Liu S-b, Zeng G-m, Jiang L, Tan X-f, et al. Adsorption of emerging contaminant metformin using graphene oxide. Chemosphere [Internet]. 2017;179:20–8. https://doi.org/10.1016/j.chemosphere.2017.03.071. (Elsevier Ltd).

49. Ghiorghita CA, Bucatariu F, Dragan ES. Sorption/release of diclofenac sodium in/from free-standing poly(acrylic acid)/poly(ethyleneimine) multilayer films. J Appl Polym Sci. 2016;133:1–9.
50. Zhang S, Dong Y, Yang Z, Yang W, Wu J, Dong C. Adsorption of pharmaceuticals on chitosan-based magnetic composite particles with core-brush topology. Chem Eng J Elsevier B V. 2016;304:325–34.
51. Fan L, Lu Y, Yang LY, Huang F, Ouyang X. Fabrication of polyethylenimine-functionalized sodium alginate/cellulose nanocrystal/polyvinyl alcohol core–shell microspheres ((PVA/SA/CNC)@PEI) for diclofenac sodium adsorption. J Colloid Interface Sci Acad Press Inc. 2019;554:48–58.
52. DavePN, Chopda L V., Kamaliya BP. Synthesis of a Polyacrylic-Grafted, MultiwalledCarbon Nanotube-Loaded Gum Ghatti Hydrogel for Diclofenac Removal. Chem EngTechnol. 2023;46:997–1004.